

Abnormal Choline Phospholipid Metabolism in Breast and Ovary Cancer: Molecular Bases for Noninvasive Imaging Approaches

Franca Podo^{1,*}, Francesco Sardanelli², Egidio Iorio¹, Rossella Canese¹, Giulia Carpinelli¹, Alfonso Fausto² and Silvana Canevari³

¹Department of Cell Biology and Neurosciences, Istituto Superiore di Sanità, Roma, Italy, ²University of Milan School of Medicine, Department of Medical and Surgical Sciences, Radiology Unit, IRCCS Policlinico San Donato, San Donato Milanese, Milano, Italy, ³Department of Experimental Oncology and Laboratories, IRCCS Fondazione Istituto Nazionale Tumori, Milano, Italy

Abstract: Elevated contents of choline phospholipid metabolites are typically detected by nuclear magnetic resonance spectroscopy (MRS) in human and animal tumors. An increase in the intensity of the ¹H-MRS profile of total choline-containing compounds (tCho, 3.2 ppm) is today considered as a common feature in different types of cancer, beyond their otherwise wide phenotypic variability. This finding fostered investigations on the molecular mechanisms underlying the observed spectral changes and on correlations between aberrant phospholipid metabolism and tumor progression. At the clinical level, efforts are addressed to evaluate effectiveness and potential use of *in vivo* localized MRS and choline-based positron emission tomography (Cho-PET) in cancer diagnosis. Aims of this article are: a) to overview recent advances in the identification of biochemical pathways responsible for the altered ¹H-MRS tCho profile in breast and ovary cancer cells, as a basis for interpreting *in vivo* MR spectra and enhanced uptake of radiolabeled choline in PET; b) to summarize recent developments of *in vivo* ¹H-MRS methods in breast cancer diagnosis; c) to discuss the potentialities of complementing current diagnostic modalities with noninvasive MRS and Cho-PET methods to monitor biochemical alterations associated with progression, relapse and therapy response in ovary cancer.

Keywords: Breast cancer, ovary cancer, choline metabolism, phosphatidylcholine cycle, ¹H-MRS, PET.

INTRODUCTION

The characterization of abnormal choline phospholipid metabolism in tumors by magnetic resonance spectroscopy (MRS) [1-5] fostered novel investigations in cancer cell biology, allowed the identification of new fingerprints of tumor progression and promoted pilot studies on clinical MRS and choline-based positron emission tomography (Cho-PET) approaches in oncology. In particular, an increase in the ¹H-MRS resonance at 3.2 parts per million (ppm), arising from the trimethylammonium headgroups of the total pool of water-soluble choline-containing metabolites (tCho), has been reported as the most common feature in a large variety of cancers such as breast [6-8], prostate [9, 10] and colon carcinomas [11], bone and soft tissue malignant lesions [12] and high-grade neuroepithelial tumors [13]. More recently, we also focused attention on alterations of the tCho spectral profile in human epithelial ovarian cancer (EOC) cells [14, 15], an aspect which received only scarce attention in the past. Our studies showed that EOC cells represent a particularly suitable model to investigate the molecular bases of aberrant choline phospholipid metabolism associated with progression of tumors of epithelial origin [15].

By comprising contributions from different phosphatidylcholine (PC) precursors and catabolites, such as phosphocholine (PCho), glycerophosphocholine (GPC) and free choline (Cho), changes in the tCho spectral profile may

result from multiple alterations in the steady state levels and fluxes of metabolites in the PC-cycle [16].

A better elucidation of the molecular mechanisms responsible for changes in the tCho resonance profile in tumor cells and tissues would pave the way to further developments in noninvasive imaging approaches for *in vivo* diagnosis and therapy response follow-up, and may also allow the identification of metabolic targets for newly designed, patient-tailored anti-tumor therapies [4, 5, 17].

This review will summarize the main results so far obtained on: a) characterization of abnormal concentrations of MRS-detectable PC metabolites in cells derived from human ovary and breast tumors, as compared to the respective non-tumoral (normal or immortalized) epithelial cells; and b) activation of different PC-cycle enzymes likely involved in the tCho spectral alterations, as a basis for interpreting ¹H-MR spectra of cancer lesions *in vivo*. An overview will then be provided on clinical ¹H-MRS methods developed in breast cancer diagnosis and on the perspectives of further extending these approaches to ovary cancer. An outline will finally be provided on the perspectives of endeavors addressed to evaluate the effectiveness of Cho-PET approaches, especially in ovary cancer.

BREAST AND OVARY CANCER: MAIN CLINICAL FEATURES AND CURRENT IMAGING METHODS

Breast Cancer

Female breast cancer is the second most common cancer in the world and the most common cancer among women, accounting for more than 400,000 cancer deaths per year. Although deaths for breast cancer are decreasing in many

*Address correspondence to this author at the Department of Cell Biology and Neurosciences, Istituto Superiore di Sanità, Viale Regina Elena 299, 00161 Rome, Italy; Tel +39 06 4990 2686; Fax +39 06 4938 7144; E-mail: franca.podo@iss.it

Western countries, breast cancer incidence rates are increasing in all regions of the world [18]. The large variation of breast cancer incidence among or within different regions may be attributed to genetic differences among populations and/or differences in lifestyle [19]. However, geographic disparities in breast cancer incidence and mortality are also related to differences in screening, chemoprevention, and treatment strategies in more-developed, as compared with less-developed regions of the world.

Furthermore, it should be taken into account that breast cancer is a clinically heterogeneous disease, and existing histological classifications do not fully capture the varied clinical course of this disease. Recent molecular approaches indicated that breast cancer is not one disease but a collection of several biologically different diseases. There are large-scale molecular differences between estrogen receptor (ER)-positive and ER-negative cancers, that reach far beyond the presence or absence of estrogen receptors. HER-2-amplified cancers also have a very distinct gene expression signature that also extends to some cancers with no apparent *HER-2* gene amplification. Further molecular categories are likely to exist in addition to and within these three most apparent molecular classes [20]. It might be useful to identify the various molecular classes because the different subsets may have a different natural history and clinical management.

Estimates from randomized clinical trials and population-based models from developed countries, such as United States and United Kingdom, indicate that early detection by screening mammography and improved treatment could result in reducing mortality rates by at least 30%. In this context, other imaging modalities could be of significant help in initial diagnosis, staging and monitoring of tumor response to treatment. For example, it should be noted that differential detection by screening mammography of ER-positive, more dormant tumors might yield an apparently higher incidence of tumors associated with more favorable survival; thus methods of functional imaging, able to identify more proliferating and aggressive tumors might be of help in programming alternative or more stringent treatment modalities. As a matter of fact, imaging beyond mammography seems recommended in the surveillance protocol of women with an increased lifetime risk of breast cancer [21-24]. Finally, early diagnosis of relapse and assessment of therapy response are vital, as they might ensure a prompt therapeutic intervention or change in treatment strategies; even in these cases a combination of functional and morphological imaging is expected to provide more sensitive and specific approaches.

Contrast-enhanced breast magnetic resonance imaging (MRI) is today the most sensitive morphological/functional technique for tumor detection and local staging of breast cancer. Breast tumors actually played an important role in the historical progress which led to the introduction of magnetic resonance imaging (MRI) in medicine. In the 1970s, when nuclear magnetic resonance rapidly converted into the most versatile imaging method, the possibility of differentiating malignant tumors from benign lesions or normal breast tissues, on the basis of relaxation times, appeared particularly promising [25]. However, when clinical

breast MRI was attempted in the early 1980s, expectations turned into rather disappointing results. In fact, classical proton density-, T1-, and T2-weighted sequences did not allow differentiation of malignant from benign tumors [26]. This scenario was dramatically changed in 1986, when Sylvia Heywang and coworkers published the first report on the use of Gd-DTPA as an intravenously administered paramagnetic contrast agent for the detection and characterization of breast tumors [27]. By exploiting the neoangiogenesis associated with tumor growth, dynamic contrast-enhanced (DCE) MRI opened an important avenue, complemented in the following years by the introduction of rapid spoiled gradient-echo sequences, dynamic acquisition and dedicated post-processing, up to the more recent approaches capable of combining high spatial with high temporal resolution [28, 29].

On the basis of these technical developments, breast MRI gained in the last decade a relevant clinical role for defined indications such as presurgical staging, diagnosis of local recurrence, evaluation of the effect of neoadjuvant chemotherapy, search of occult primitive breast tumor in patients with metastases and surveillance of women at familial-genetic high risk of breast cancer. These results were due to a top level sensitivity (about 95% for invasive cancers) and to an increasing specificity, estimated to be at least 75-80% when morphologic and dynamic criteria are integrated in a unique evaluation system. The remaining gap between sensitivity and specificity is filled-in by second look ultrasound (US) examination and MRI-guided breast biopsy.

In the meanwhile, the introduction of *in vivo* localized MRS approaches opened the way to a powerful complementation of the anatomical/physiopathological information provided by conventional imaging modalities, by adding metabolic information potentially useful to enhance diagnostic accuracy and to offer noninvasive assessment of novel biomarkers of *in vivo* tumor progression [3, 4, 6, 17]. The additional information provided by MRS may therefore substantially contribute to improve pre-operative assessment of tumor aggressiveness and to monitor early tumor response *in vivo*.

Early *in vitro* ^{31}P -MRS studies demonstrated altered phospholipid metabolism in cancer cells, by detecting increased levels of phosphomonoesters such as PCho and phosphoethanolamine and, sometimes, also their phosphodiester analogues, GPC and glycerophosphoethanolamine [2, 3]. Despite an *in vivo* dependence of the ^{31}P spectrum on hormonal status [30], the results of ^{31}P -MRS for differentiating malignant from benign breast tumors were found inadequate for a clinical use [31]. On the contrary, in the last decade, many *in vivo* ^1H -MRS studies based upon tCho signal analysis in breast cancer lesions offered promising results with possible translation into clinical practice [32-35], as discussed in more detail in a following section. This perspective was also strengthened by the possibility to perform a ^1H -MRS study as a final step after a regular breast DCE-MRI examination.

In comparison with conventional imaging techniques such as computed tomography (CT), US and MRI, PET with fluoro-18 fluorodeoxyglucose (^{18}F -FDG), used as such or in combination with CT (PET/CT), offers the advantage of a

high sensitivity in detecting metabolic abnormalities of tumor lesions and contributes to breast cancer staging mainly in terms of identification of bone [36] and lymph node metastases.

Ovary Cancer

EOC has a relatively low incidence (approximately 1/100,000 new cases each year) in North America and in Europe and up to 10-fold lower incidence rates are observed in most parts of Africa and Eastern Asia; furthermore, within a particular country, incidence rates may differ among ethnic groups [37]. Despite the low incidence, epithelial ovarian cancer presents a high case-fatality ratio and is the most lethal gynecological malignancy in industrialized countries, with an overall 5-year survival still remaining at about 44% [38]. The unfavourable statistics in ovarian cancer patients reflects in part the poor understanding of the molecular pathogenesis and progression of this heterogeneous malignancy. Although much remains to be discovered, numerous gene alterations have been identified as associated to this disease [39, 40] and a model of development has been recently proposed [41]. Women with organ-confined tumors have an excellent prognosis, but the majority of early stage cancers is asymptomatic and more than two-thirds of patients are diagnosed with advanced disease. Initial surgery is almost always necessary in the management of suspected ovarian cancer for histological confirmation, staging and tumor debulking. Effective cytoreductive surgery at the time of diagnosis, achievable mainly in early-stage disease, has been correlated with improved survival. However, due to the difficulties in early diagnosis, the vast majority of EOC patients require adjuvant treatment in the attempt to eradicate residual disease. EOC is considered to be a chemosensitive tumor and the median overall survival significantly improved after the development of new therapeutic approaches. About two-thirds of EOC patients who receive highly active front-line chemotherapy enter clinical remission, but relapse occurs in the majority of advanced-stage patients even after complete response to initial treatments.

According to the Federation of Gynecologists and Obstetrics (FIGO), staging criteria in post-surgical treatment and follow-up, radiological tests such as US, CT or MRI should only be performed when clinical findings or a raise in serological tumor markers (CA-125) suggest a possible recurrence. However, due to the tumor location in the abdominal and pelvic peritoneum and the propensity for diffuse small-volume disease, recurrent EOCs are clinically detected and located in most patients when the lesions are larger than about 2 cm; alternatively, invasive procedures (second-look laparotomy) should be adopted [42]. The positive prognostic impact of early diagnosis of relapse (detection of small lesions less than 0.5 cm) as well as of the assessment of response at the end of treatment could be fully exploited only if noninvasive *in vivo* imaging techniques with high sensitivity and specificity are successfully applied.

The role of imaging is to detect and characterize adnexal masses as likely malignant, recognize unusual findings that may suggest a typical pathology, demonstrate metastases in order to prevent under-staging and detect a specific size of disease that may be unresectable [43]. A strategy for diagnosis of ovarian benign, borderline malignant and

malignant masses with MRI incorporates signal intensity characteristics into morphologic features [44].

A retrospective study showed that gadolinium-enhanced spoiled gradient-echo MRI depicted residual tumor in women with treated ovarian cancer with an accuracy, positive predictive value and negative predictive value that were comparable with those of laparotomy reassessment and superior to those of serum CA-125 values alone [45]. However, the specificity of MRI of the pelvis may be substantially limited by the presence of post-surgical anatomical alterations. On the other hand, ^{18}F -FDG-PET has been found to be very sensitive in detecting recurrent or persistent ovarian cancer [46], while the combined functional-anatomic imaging given by PET/CT may substantially improve sensitivity and specificity of imaging studies [47, 48]. However, false-negative ^{18}F -FDG PET imaging of tumors of the reproductive tract or misinterpretation of metastatic involvement of lymph nodes may derive from artifacts associated with physiologic accumulation of the radiotracer in the urinary route [49]. These considerations suggest the interest of further investigating the potentialities of alternative imaging approaches in ovarian cancer, such as *in vivo*-localized MRS and Cho-PET, especially for the discrimination of scars from recurrent disease and evaluation of therapeutic response.

EVIDENCE AND MOLECULAR BASES OF ALTERED CHOLINE METABOLISM IN BREAST AND OVARY CANCER CELLS

Abnormal Levels of Choline Metabolites

Quantitative high-resolution ^1H -MRS analyses at high field allowed us to measure a tCho content of 5.2 ± 2.4 nmol/ 10^6 cells (corresponding to a cellular average concentration of about 2.0 mM) in aqueous extracts of normal ovary surface epithelial cells or their immortalized non-tumoral cell variants (EONT) [15]. With respect to this basal level, the tCho content measured in different EOC cell lines (SKOV3, OVCA432, CABA I, IGROV1, OVCAR3) reached much higher intracellular levels (4.0 to 7.0 mM). The most remarkable feature was a 3.0- to 8.0-fold increase in PCho in EOC with respect to EONT cells. Fig. (1) shows a typical example of increased intensity and altered composition of the tCho spectral profile in a EOC cell line as compared to normal cells. The average percent contribution of this metabolite to the overall tCho resonance profile increased from about 50% in EONT to 70-90% in EOC cells. In parallel, the GPC/PCho ratio underwent a ten-fold decrease (a phenomenon already reported for some oncogene-transformed and cancer cells, and known as the “GPC-to-PCho switch” [6, 50]).

Significant increases in tCho and PCho ($P < 0.05$) have also been reported for tumorigenic, highly metastatic breast cancer cell lines (such as MDA-MB 435; MDA-MB 231) as compared to human mammary epithelial cells (HMEC) and their immortalized non-tumoral cell variants [6, 9]. In fact, the overall computed concentration of tCho increased from about 0.2 mM in HMEC to 2–4 mM in breast cancer cells, with an average PCho contribution of about 80% to the tCho spectral profile. It is worth noting that MRS analyses of aqueous extracts of samples isolated from breast cancer

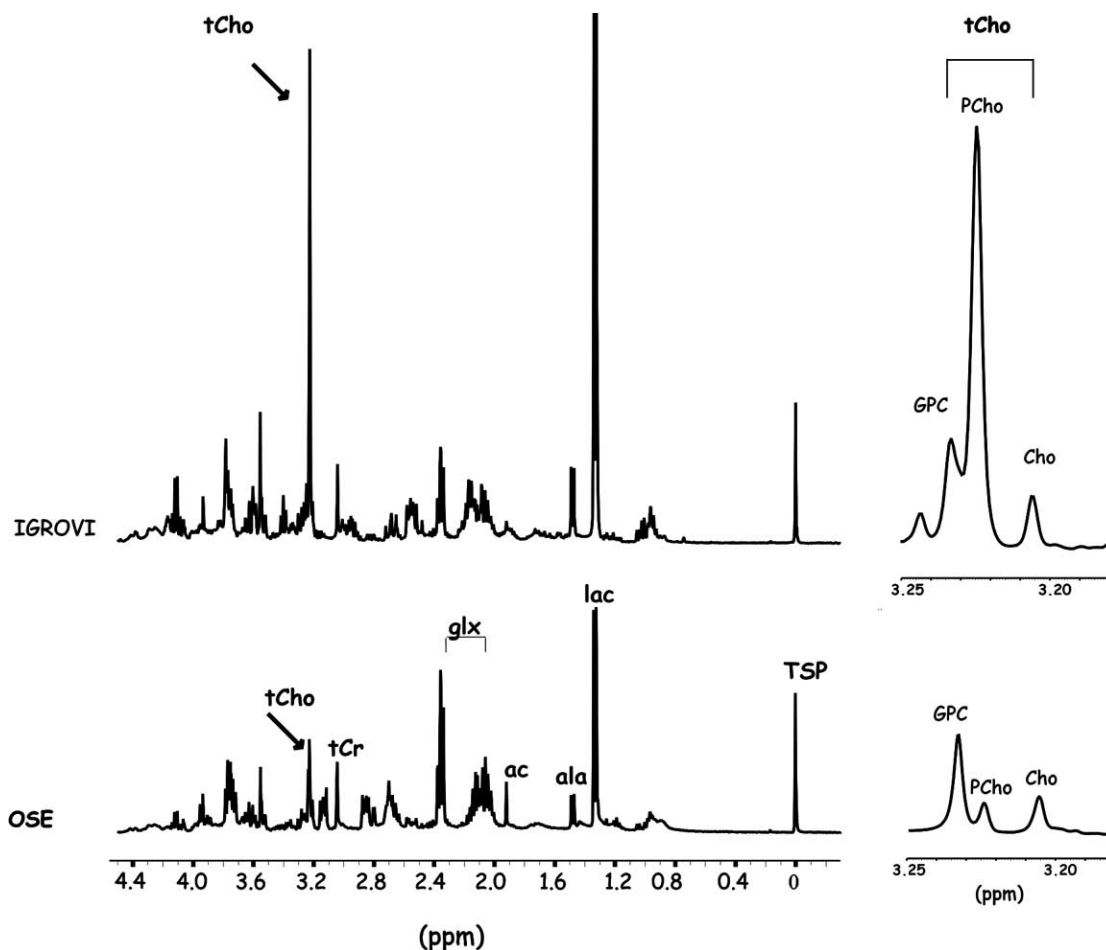


Fig. (1). Left: Typical examples of ^1H MR spectra (9.4 T) of aqueous extracts of an epithelial ovarian cancer cell line (IGROVI) and non-tumoral ovarian surface epithelial cells (OSE). Right: expanded spectra (16.5 T) of the tCho resonance profile (3.2 ppm). Peak assignments: tCho, total choline-containing metabolites; GPC, glycophosphocholine; PCho, phosphocholine; tCr, creatine and phosphocreatine; glx, glutamine and glutamate; ac, acetate; lac, lactate; TSP, trimethylsilylpropionate (reference).

lesions and non-involved breast tissues confirmed that the average total amount of tCho was more than ten-fold higher in tumors [51].

The observed changes in PCho contents in both breast and ovary cancer cells with respect to their normal or non-tumoral immortalized counterparts, did not correlate with differences in cell doubling time [6, 15]. This finding represents an important issue in the elucidation of molecular mechanisms associated with altered choline metabolism in cancer. Against previous assumptions (reviewed in ref 3), the present body of evidence supports the general hypothesis that an increased PCho concentration is not a simple indicator of incremented phospholipid production (necessary to cancer cells to cope with higher proliferation requirements), but more likely results from activation of different PC-cycle enzymes, under genetically induced changes in growth factor-mediated cell signaling pathways [6, 16, 17].

The alterations measured in steady-state contents of different choline phospholipid metabolites allowed a clear-cut discrimination ($P < 0.0001$, within 95% confidence limits) of EOC from EONT cells, on the basis of two-dimensional metabolic maps constructed by plotting either the PCho/tCho

or the GPC/tCho ratio *versus* the absolute tCho concentration. This striking separation of EOC from EONT into independent metabolic clusters, together with the prevalent contribution of PCho to the tCho profile, supports the value of utilizing ovarian carcinoma cell lines as a model for further investigating the biochemical mechanisms responsible for these MRS-detected metabolic features in epithelial cancer cells [15].

Activation of Phosphatidylcholine-Cycle Enzymes

The observed increases in intracellular PCho content in ovary and breast cancer cells may in principle result from activation of different biosynthetic and/or catabolic PC-cycle pathways [16] as outlined in Fig. (2).

The major enzymes which may contribute to alterations in the intracellular pools of different PC precursors and catabolites, such as PCho, GPC and Cho, are shortly discussed.

The *de novo* biosynthesis of PC occurs *via* the three-step Kennedy pathway (also known as cytidyldiphospho-choline (CDP-Cho) pathway) in which choline is phosphorylated into PCho by choline kinase (Chok), PCho is converted into CDP-choline by cytidylyltransferase (ct) and CDP-choline is

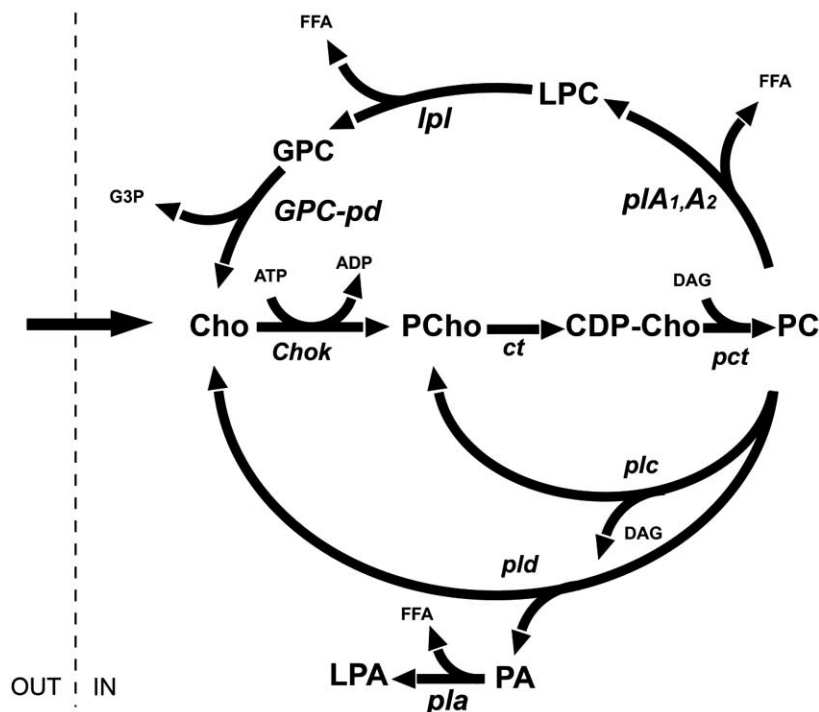


Fig. (2). Schematic representation of phosphatidylcholine (PC) *de novo* biosynthesis and catabolism. *Metabolites*: CDP-Cho, cytidine diphosphate choline; Cho, choline; DAG, diacylglycerol; FFA, free fatty acid; G3P, *sn*-glycerol-3-phosphate; GPC, glycerophosphocholine; LPA, lyso-phosphatidate; PA, phosphatidate; PCho, phosphocholine. *Enzymes*: Chok, choline kinase (EC 2.7.1.32); ct, cytidyltransferase (EC 2.7.7.15); lpl, lysophospholipase (EC 3.1.1.5); pct, phosphocholine transferase (EC 2.7.8.2); pd, glycerophosphocholine phosphodiesterase (EC 3.1.4.2); plA₂, phospholipase A₂ (EC 3.1.1.4) and plA₁, phospholipase A₁ (EC 3.1.1.32); pla, phospholipase a; plc, phospholipase C (EC 3.1.4.3); pld, phospholipase D (EC 3.1.4.4).

incorporated into PC by choline phosphotransferase (pct) [52]. While ct mediates the rate-limiting step of the pathway, Chok acts as a regulatory enzyme for PC biosynthesis. As an example of Chok regulation, the intracellular activity rate measured for this enzyme in 3T3 fibroblasts (1.2 ± 0.2 nmol/10⁶ cells·h) undergoes a 2- to 3-fold increase following growth factor-induced cell stimulation [53] or H-*ras* transformation [54].

The Chok activity measured in our laboratory in EONT cells was only 0.6 ± 0.1 nmol/10⁶ cells·h but increased 12- to 24-fold ($P < 0.001$) in EOC cells [15].

The increases in Chok activity and PCho levels in EOC cells are in agreement with a substantial body of evidence reported in the literature on implications of this enzyme and its choline-containing product in human carcinogenesis. Elevated Chok activity has been reported in a variety of cancers, including lung, colon and prostate tumors [55] and in breast carcinomas [56]. Moreover, Chok activation has been found in about 40% of breast tumor tissues, in which it was associated with clinical indicators of increased malignancy, such as high histologic tumor grade and ER-negative status [56]. In addition, Chok overexpression/activation has been shown to be a critical requirement for the proliferation of human mammary epithelial cells (HMEC) and for breast tumor progression [57], while a specific Chok inhibitor (MN58b) efficiently blocked receptor-induced proliferation of *in vitro* cultured breast tumor cells and inhibited their *in vivo* growth in animal models [57, 58]. In

general agreement with the reported overexpression and increased activity of Chok in malignant cells and tumors, RNA-interference-mediated Chok suppression in breast cancer cells induced cell differentiation and reduced *in vitro* cell proliferation [59].

In this context, the different rates of Chok activity measured in EOC and EONT cells warrant further investigations to elucidate to which extent activation of individual isoforms of this enzyme [60] may act as possible pharmacodynamic endpoints of new cancer therapies, either based upon specific Chok inhibition [61] or upon selective targeting against cell signaling pathways involved in Chok regulation.

An important implication of enhanced Chok activity in breast and ovary cancer cells is the expected increase in the phosphorylation of a radiolabeled choline tracer transported from the medium into intracellular compartments. *In vitro* measurements on uptake of ¹⁴C-choline by ovary epithelial cells [15] actually showed that the incorporation of this radiotracer into the cells was (within 1 hour) 5- to 15-fold higher in EOC than in EONT cells ($P < 0.0001$). Recent analyses by Yoshimoto *et al* [62] showed 1.5- to 4.0-fold increases in the average [¹⁴C]-Cho uptake by a wide variety of cancer cells as compared to non-tumoral fibroblasts, with a radiolabel distribution mainly confined (within 45 min) to water-soluble choline metabolites. In fact, ¹⁴C-PC reached, in this time window, levels lower than 5% of the total pool of ¹⁴C-labeled compounds. Moreover, [¹⁴C]-Cho uptake

correlated with Chok activity and with [^3H]-thymidine incorporation (a well known index of cell proliferation). Similar mechanisms and rates of radiolabeled choline uptake and accumulation into water-soluble PC precursors of tumor cells can be predicted to take place in ^{11}C - or ^{18}F -Cho PET examinations [63, 64] of ovary cancer cells *in vivo*, and could form the basis for the prediction of differential standard uptake (SUV) ranges for normal and malignant tumor lesions, following a bolus administration of the radiotracer. It is worth emphasizing that, according to these *in vitro* uptake analyses [15, 62], the “metabolic window” of *in vivo* PET examinations is mainly confined to Cho transport and phosphorylation in the Kennedy pathway, the higher SUV values of radiolabeled Cho in tumors most likely reflecting increased cell proliferation.

On the other hand, regarding the biological meaning of MRS signal variations, multiple pathways may contribute to the enhanced PCho levels detected under the tCho profile of tumor cells. In fact, although Chok activation likely represents a key issue in the interpretation of abnormal PCho contents in EOC cells, no statistically significant correlation was found between Chok activity rates and PCho levels detected in the different EOC cell lines investigated [15]. This result suggests the interest of further investigating the role of both biosynthetic and catabolic PC-cycle pathways in PCho accumulation in cancer cells.

Three major catabolic pathways can contribute to the formation of a MRS-detected intracellular PCho pool: PC hydrolysis into PCho and diacylglycerol, mediated by a specific phospholipase C (PC-plc); combination of phospholipase D (pld)-mediated PC degradation into Cho and phosphatidate and further Cho phosphorylation by Chok into PCho; phosphodiesterase (pd)-mediated hydrolysis of GPC into Cho and glycerophosphate and subsequent Cho phosphorylation [65]. The last reaction represents the terminal step of PC degradation along the deacylation pathway mediated by the combined action of phospholipases A_2 and A_1 and lysophospholipases (lpl).

Assays on PC catabolism carried out in our laboratory by measuring Cho formation in total cell lysates of EONT and EOC cells following addition of a monomeric, short-chain PC (1,2-dihexanoyl-*sn*-glycero-3-phosphocholine, C6PC) showed that PC-plc activity increased 9- to 15-fold in EOC cells, while pld was only activated about 2- to 3-fold in some, but not in all EOC cells and GPC-pd activity increased about 2- to 4-fold ^(1,2). Furthermore, Western blotting and confocal laser scanning microscopy experiments showed that PC-plc activation in EOC cells is associated with massive expression of this enzyme on the outer plasma membrane surface of EOC cell lines, as well as on that of cells isolated from patient ascitic exudates ⁽¹⁾.

The overall body of results overviewed in this section shows that both biosynthetic and catabolic PC-cycle

pathways may contribute to the increased MRS-detected PCho levels in cancer cells, while increased radiolabeled Cho uptake in PET examinations is mainly due to Cho transport into the cell and subsequent phosphorylation in the Kennedy pathway.

^1H MRS OF BREAST CANCER

Background

A number of *in vivo* localized ^1H -MRS clinical studies conducted in the last decade reported increases in the area of the tCho peak detected in primary breast tumors larger than 1 cm of diameter [66-82], supporting the proposal that this spectral parameter may represent a useful biomarker for noninvasively testing malignancy in breast lesions.

Fig. (3) shows an example of *in vivo* ^1H -MRS examination of an infiltrating ductal carcinoma compared with healthy gland tissue in the same breast.

When ^1H -MRS was integrated in a complete imaging protocol, it was reported to improve the specificity of breast MRI [77] and was suggested as a useful adjunct to MRI for reducing the number of lesions proposed for biopsy on the basis of MRI examinations alone [82]. Moreover, preliminary results of an inter-observer performance study at 4.0 T [80] showed that addition of ^1H -MRS to MRI significantly improved the radiologist ability to distinguish benign from malignant breast lesions.

The potentiality of *in vivo* and *in vitro* MRS analyses in the evaluation of nodal status was investigated, with promising results, in patients with breast cancer, using choline metabolites as biomarkers for metastasis [83-85].

Furthermore, decreased levels of choline-containing metabolites were reported in tumors following response to neoadjuvant therapy [70].

Technical Aspects and Interpretation

The most commonly used ^1H MRS approach in breast cancer diagnosis and follow-up is single voxel spectroscopy (SVS). The application of multivoxel two-dimensional chemical shift imaging (CSI) methods is still in a preliminary, although very promising phase [78, 81].

The SVS approach is based upon the acquisition of a single spectrum acquired from a single voxel corresponding to the volume of interest (VOI) positioned on the MRI-detected lesion, usually a contrast-enhancing mass. This VOI is spatially defined using images obtained or reconstructed along the three orthogonal planes. The VOI should exactly comprise the mass to be examined, limiting as much as possible contamination from surrounding tissues, particularly from fat. This method requires previous identification of the lesion by DCE-MRI and takes advantage of the lack of any significant relaxation effect induced by the paramagnetic agent on the ^1H -MRS tCho signal [69], probably due to the basically different location of choline metabolites (intracellular space) and Gd-chelates (vascular and extracellular space).

According to our *in vivo* experience using a 1.5 T unit (Sonata, Siemens, Erlangen, Germany), before applying a SVS ^1H -MRS sequence, it is important to optimize the local

¹Iorio E, Ricci A, Mezzanzanica D, Spadaro F, Ramoni C, Canese R, Rozera C, Spada M, Belardelli F, D'Ascenzo S, Dolo V, Canevari S, Podo F. Choline phospholipid metabolism in human ovarian tumor progression: a MRS study. In: *Proceedings Intl Soc Mag Reson Med* 2006; 3181.

²Iorio E, Ricci A, Pisanu ME, Di Vito M, Canese R, Mezzanzanica D, Canevari S, Podo F. Activation of PC cycle enzymes in human epithelial ovarian carcinoma cells. *Magn Reson Mat Phys Biol Med (MAGMA)* 2006;19(Suppl 1):50.

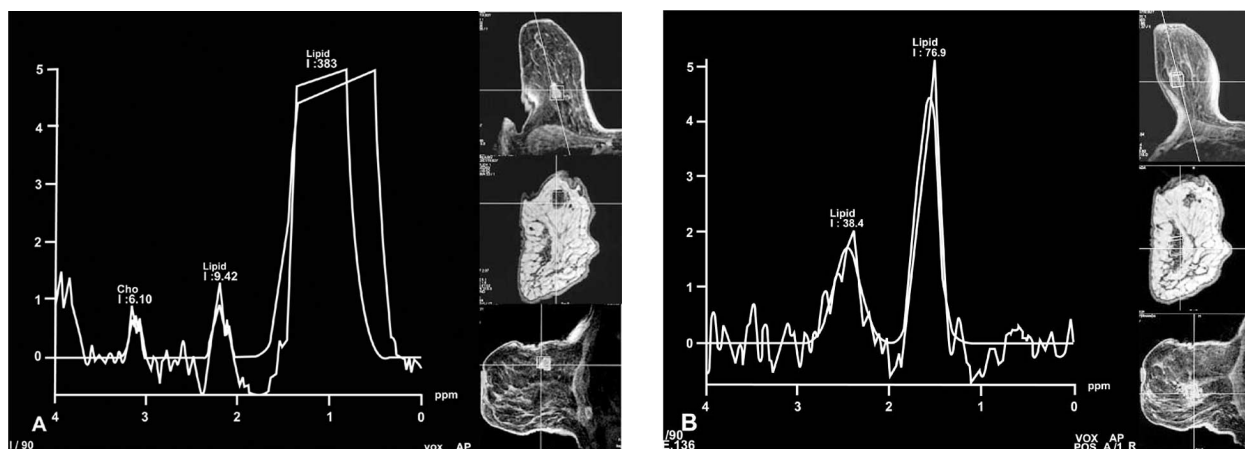


Fig. (3). Comparison between an infiltrating ductal carcinoma (A) and healthy gland tissue (B) of the same breast (*in vivo* single-voxel ^1H -MRS - PRESS sequence, TE 136 ms - after Gd-enhanced dynamic study at 1.5 T). On the right of both spectra, three images obtained on orthogonal planes (from top to bottom: postcontrast subtracted axial, precontrast coronal, reformatted postcontrast subtracted sagittal) with indication of the selected volume of interest (VOI, about 2 cm^3 for both the tumor and the healthy gland tissue). Note the evident total choline peak (3.2 ppm, integral = 6.1 arbitrary units) for the tumor and the absence of a detectable peak, in the same spectral interval, for the healthy gland tissue.

field homogeneity by means of a software-guided *shimming* procedure and to verify the effectiveness of pre-pulses utilized for water and fat signals' suppression. Specific pulses are in fact dedicated to reduce as far as possible the resonances arising from these molecules, largely present in breast tissues (in particular, the water peak in the 4.2 to 5.2 ppm spectral region, with central frequency at 4.7 ppm, and the major fat peaks in the regions 0.0 – 2.5 ppm and 5.1 – 5.7 ppm). In the absence of this procedure, the remaining metabolites would be practically undetectable.

The most commonly used SVS sequences are *point-resolved spectroscopy* (PRESS) or *stimulated echo acquisition mode* (STEAM). The signal intensity is higher (about double) in PRESS than in STEAM. However, STEAM is less sensitive to modulations of signal intensity by J-coupling between nuclear spins, and allows application of more effective techniques of water and fat suppression [86].

As typical of MR measurements, a larger number of excitations (NEX) leads to a higher signal-to-noise (S/N) ratio, at the cost of a longer acquisition time. In our clinical experience using a PRESS sequence, acquisition of spectra of good quality for a VOI of at least 1 cm^3 requires 512 NEX. As a consequence, the acquisition time is near 13 min⁽³⁾. Post-processing is performed using relatively standardized protocols including several steps before/after Fourier transform, such as application of filters (exponential, gaussian, Hanning's, rectangular); frequency, phase, and baseline correction; and curve fitting for spectral profile optimization. An appropriate software then provides peak labeling and integration.

The detection of tCho in the 3.14-3.34 ppm spectral region is related to malignancy of tissues in the selected

VOI. In this spectral range a number of metabolites are detected, including Cho, PCho, GPC, myoinositol, and taurine, whose contributions to the tCho spectral profile are difficult to separate at 1.5 T. Some authors adopted a S/N threshold of 4.0 for the tCho signal, measuring the noise in the 7.0 to 9.0 ppm spectral region (where no peaks are detected) [81]. A relevant contribution to the analysis of the tCho peak has been recently given by Stanwell and coworkers [79], in a study at 1.5 T on 43 asymptomatic volunteer women (including three breast feeding mothers) compared with 21 breast cancer patients. Using a particular post-processing program optimized for spectral resolution, the diagnostic specificity could be improved from 80% to 100%, by discriminating breast malignant tumors from three false-positive and the three lactating breasts, on the basis of the different position of the tCho central frequency. In fact the tCho signal was found to be shifted from 3.22 ppm (consistent with PCho) in tumors to 3.28 ppm (possibly due to myoinositol, taurine and GPC) in the breast of false-positive volunteers or lactating mothers. Moreover, in one third of the malignant tumors, the tCho profile centered at 3.22 also comprised signal components at 3.28 and 3.04 ppm (the latter being the typical frequency of creatine and phosphocreatine) [79].

Finally, the possibility of absolute quantification of tCho has been demonstrated *in vivo* both at 1.5 T and 4.0 T [67, 71, 76, 80]. The lowest detectable level of tCho reported at 1.5 T was 0.2 mM (echo time 31 ms, 1 cm resolution) [67], while a concentration of 2.0 mM was first reported for a breast cancer lesion *in vivo* by Bakken *et al.* [71], in agreement with *in vitro* measurements. Absolute quantification at 4.0 T reported by Meisamy *et al.* [80] using a method developed by Bolan *et al.* [76] showed that the tCho level in malignant lesions ranged from 0.0 to 8.5 mM (mean value 2.2 mM), as compared to a range of 0.0 - 1.1 mM (mean 0.21 mM) in benign lesions.

³ Fausto A, Sardanelli F. Value of proton spectroscopy added to a highly spatially resolved Gd-enhanced MR study of the breast. Proceedings 91th RSNA 2005: 177.

More detailed information on the individual metabolites contributing to the *in vivo* tCho spectral profile (with evidence on the prevalence of the PCho component) could be obtained by *ex vivo* (or *in vitro*) high resolution ^1H MRS analyses of breast tumor specimens (or their aqueous extracts) [51, 87-89]. Among these approaches, the technique of high resolution magic angle spinning (HR MAS) is particularly powerful. In fact, it allows comparative examination of the tCho spectral profile of a given cancer lesion *in vivo* with that of its fine-needle or surgical biopsies analysed *ex vivo* at a resolution comparable to that of conventional ^1H -MRS analyses on cell extracts [90], whilst maintaining the possibility of further histological analysis of tissue samples [89]. The HR MAS approach is based on the application of a rapid spinning to an intact tissue sample around the so-called magic angle ($54^\circ 44'$), whereby line broadening typical of semisolid or solid compartments is reduced to values comparable with that of slightly viscous liquids [91]. A combination of one- and two-dimensional HR MAS ^1H MRS methods led to reproducible detection and assignment in breast cancer tissues of over thirty different metabolites, including that of choline-containing compounds [92]. Fig. (4) shows an example of HR MAS ^1H MR spectral profile of the tCho resonance in a large-core biopsy from an infiltrating ductal carcinoma. Integration of *in vivo* and *ex vivo* MRS approaches are expected to improve the accuracy of MR in breast cancer diagnosis and staging.

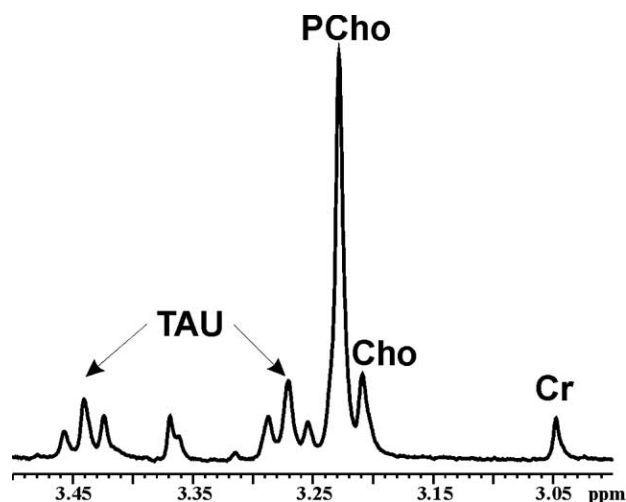


Fig. (4). ^1H MRS tCho profile detected by high resolution magic angle spinning (HR MAS) analysis at 9.4 T in a tissue sample isolated from a large-core biopsy of breast primary infiltrating ductal carcinoma.

Clinical Results

Clinical studies using ^1H -MRS to characterize breast lesions showed interesting results, even though the number of patients enrolled by each of them was relatively low. A meta-analysis by Katz-Brull and coworkers in 2002 pooled the results of five studies published between 1998 and 2001, concerning a total of 153 breast tumors, one hundred of them referred to histologic analysis as the gold standard [73]. The sensitivity of ^1H -MRS resulted to be 83% (CI 95%, 73–89%)

and the specificity 85% (CI 95%, 71%–93%). However, excluding technically inadequate measurements (low signal-to-noise ratio), both sensitivity and specificity reached 92%. The limit of this analysis is the obvious inhomogeneity of inclusion criteria, spectroscopic sequences and post-processing.

Our direct experience confirmed the value of combining ^1H -MRS with DCE-MRI of breast lesions^(3,4). We considered a series of 244 consecutive patients studied (from January 2003 to November 2004) by breast DCE-MRI at 1.5 T using a voxel of 1 mm^3 . One hundred eighteen patients had a negative result (no enhancing lesions or enhancing foci less than 5 mm in diameter) and two patients interrupted the examination. In the remaining 124 patients we performed 151 SVS ^1H -MRS acquisitions using PRESS sequence (TR/TE=1500/136 ms) with a mean voxel of $2.9 \pm 2.2\text{ cm}^3$ (range 1–8 cm^3) and a mean acquisition time of about 13 min. A technically inadequate spectrum (low signal-to-noise ratio) was obtained in three patients due to movement artifacts. The gold standard was histological examination after surgical excision for lesions scored as BI-RADS [93] 4 or 5, core-biopsy or 1-year follow-up for those scored as BI-RADS 2 or 3. Using a threshold of 2.0 for the tCho peak integral (retrospectively defined on the first 17 cases, under internally standardized instrumental conditions), the sensitivity of ^1H -MRS was 90% (equal to the sensitivity of the dynamic contrast-enhanced MRI study) while specificity was higher (89%) than that of DCE-MRI (81%). The results indicated that a gain in specificity of 8% could be obtained thanks to ^1H -MRS. The trade-off of this gain was paid in terms of a longer time of MR examination, prolonged for only about 15 min, with a total examination time for breast DCE-MRI and MRS of about 30 min. Importantly, excluding the lesions smaller than 10 mm in diameter (for which a contamination by breast tissues surrounding the lesion is likely) ^1H -MRS reached a sensitivity of 97%.

Clinical perspectives of ^1H -MRS of the breast are not exclusively limited to lesion characterization. The tCho peak already disappeared or decreased in early phases of neoadjuvant chemotherapy in 89% of locally advanced tumors which showed the tCho peak before treatment [70]. In the evaluation of nodal metastases, ^1H -MRS, compared with fine-needle aspiration cytology of suspicious nodes, showed a sensitivity of 82% and a specificity of 100% (accuracy 90%) [83]. Finally, an interesting correlation between the tCho tumor concentration and the presence of metastatic lymph nodes was demonstrated at 4 T⁽⁵⁾.

^1H MRS OF OVARY CANCER

According to multivariate analysis of ^1H MRS spectra of *ex vivo* biopsy specimens isolated from ovarian cancer lesions [94, 95], the tCho spectral region was identified as one of the important classification regions (3.3, 3.2, 3.0, 2.8, 1.7, and 1.5 ppm) relevant to discrimination between benign

⁴ Fausto A, Iozzelli A, Sardanelli F. Isotropic high resolution (1-mm³) MR dynamic imaging and single-voxel proton spectroscopy of the breast. An effective way to present morphology, dynamics, and metabolism of breast lesions. *Eur Radiol* 2004; 14 (Suppl 2): 382.

⁵ McIntosh A, Bolan PJ, Meisamy S, et al. Using quantitative choline measurements to predict axillary node status in human breast cancer, *in vivo*. *Proceedings Intl Soc Mag Reson Med* 2005: 132.

and malignant tissue samples. These findings suggested the interest of focussing on the identified spectral regions in future ^1H MRS analyses of ovarian tumors *in vivo*. Moreover, significantly higher levels of choline metabolites ($P = 0.0009$) were found in malignant (mean value $42 \mu\text{mol/L}$; range $19\text{--}113 \mu\text{mol/L}$) than in benign cyst fluids (mean value $15 \mu\text{mol/L}$; range $>2\text{--}163 \mu\text{mol/L}$) [96].

In vivo MRS is still at its infancy for ovarian cancer and, accordingly, few clinical reports are available from literature search. In two different studies, both evaluating a limited number of large lesions or tumors of the female pelvis, different metabolites (Cho, lactate, lipids and creatine) were measured by single-voxel proton MRS. The use of this approach showed significant differences in metabolites' concentrations between benign and malignant ovarian tumors and pelvic abscesses. Interestingly, the tCho signal was found only in ovary carcinoma, suggesting a potential clinical application of this methodology [97, 98].

Our pioneering clinical experience with the application of a 3D multi-voxel ^1H MRS protocol allowed a clear detection of the tCho peak in malignant areas of an adnexal mass *in vivo* (Fig. (5)).

Our experience was also extended to preclinical models of human ovary cancer, in which the detection of a high tCho peak represented a spectral feature of both orthotopic and heterotopic cancer lesions, obtained by either intrapelvic or subcutaneous injection of human ovary carcinoma cells in immunodeficient mice (Fig. (6)). The use of these models appears of particular interest for investigating the correlations between the tCho resonance and other biological characteristics of the ovary tumors [99] and for evaluating

the use of this signal as possible surrogate biomarker of cancer response to conventional or innovative therapies [100–102].

METABOLIC IMAGING BY PET

General Background

A molecular imaging method such as PET can establish metabolic or functional parameters of tissues and may help to distinguish between viable tumor masses and masses consisting of necrotic or scar tissue. The PET principles, instrumentation and methodological considerations are excellently described in recent reviews [103–106]. Major advantages of PET over conventional imaging methods are the ability to convey functional information and the possibility to provide quantitative information on regional radio-pharmaceutical concentration. Another strength of PET, as compared to other radiotracer imaging methods such as single-photon emission tomography (SPECT), is the possibility to utilize a wide range of radiopharmaceuticals. PET radiotracers are based on isotopes such as fluorine (^{18}F) and carbon (^{11}C); they strongly differ in the half-life of positron emission (respectively 110 and 20 min), so that ^{11}C -PET requires in-house radiotracer production and has a limited imaging time-frame. Apart from the isotope characteristics and the chemical procedure needed for radiolabeling, the final choice of the radiotracer is mainly dictated by its availability, the known physiological fate of the metabolite and the expected alteration in its metabolism in tumor cells. Accordingly, the most commonly used radiotracer in routine clinical applications is FDG, a radiolabeled glucose analog that allows monitoring of increased glucose metabolism in

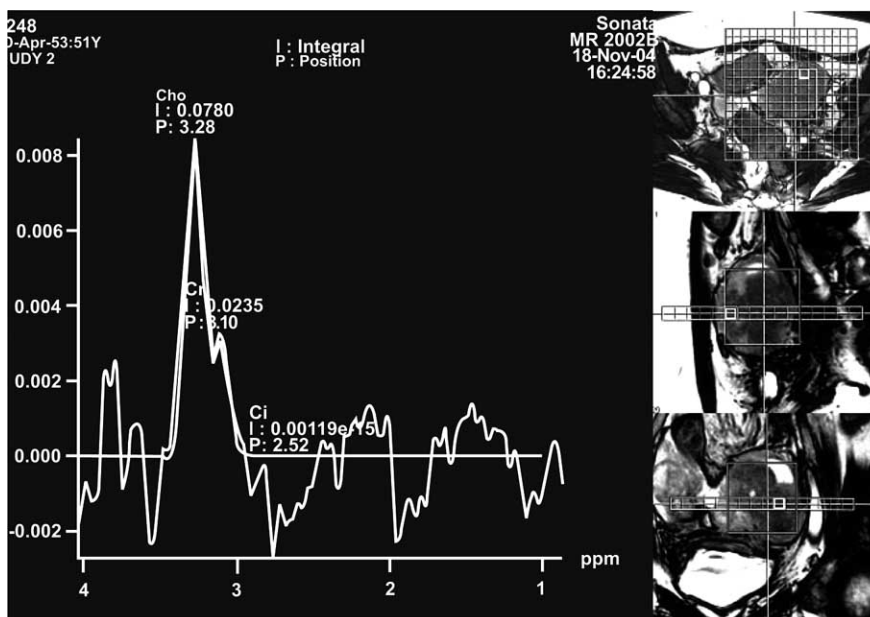


Fig. (5). 3D multivoxel ^1H -MRS of an epithelial tumor of the left ovary at 1.5 T (STEAM sequence, TE 120 ms). On the right of the spectrum, three images obtained on orthogonal planes (from top to bottom: axial, sagittal, and coronal) with superimposition of the global VOI subdivided into multiple slices. Each slice was further subdivided in multiple small voxels, each of them associated with a single spectrum. The spectrum was obtained from the voxel indicated by the small white-boldd square. The scanning resolution is about 1.7 cm^3 . The total choline peak (3.2 ppm) is well depicted as the highest one in the spectral interval shown here. However, the value of the peak integral is about 100 times smaller than that shown for the case of single-voxel ^1H -MRS of the breast tumor in Fig (3) A. This is due to the different size of the volume resolved using the two ^1H -MRS techniques.

Ovarian carcinoma (OVCA 432) in SCID mice

intraperitoneum subcutaneous

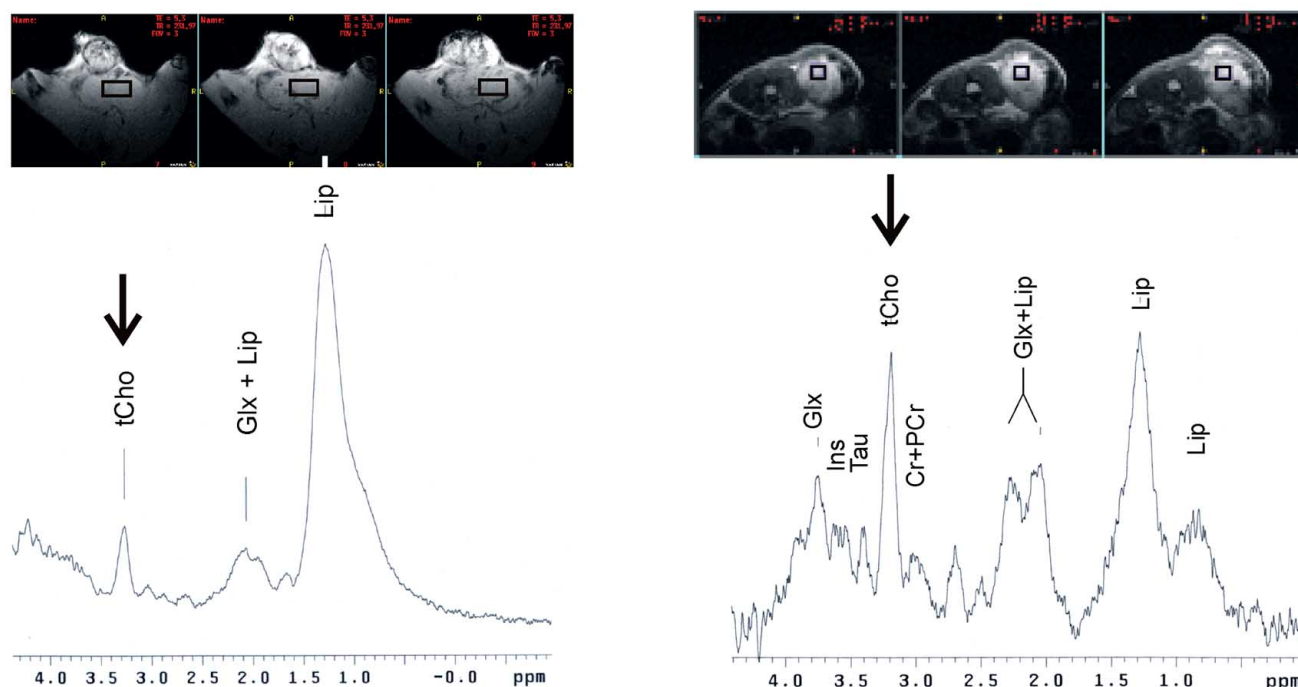


Fig. (6). Examples of MRI and ^1H -MRS analyses (4.7 T) of intraperitoneal (ip) and subcutaneous (sc) xenografts of human ovary cancer cells (OVCA432) in SCID mice. ^1H MR images and spectra were obtained about 50 days after ip or sc injection of 10^6 cells. Transverse images were obtained with a gradient echo technique (TR/TE=183/5.3 ms, $\alpha = 20^\circ$, 15 contiguous slices, 1 mm thickness, FOV = 30 x 30 mm, matrix 128 x 128, corresponding to in plane resolution of 0.23 x 0.23 mm, 2 averages). ^1H MR spectra were acquired from the voxels indicated in the respective images, by using a PRESS sequence (TR/TE = 1500/23 ms, ROIs ranging from 8 to 40 μl , number of averages ranging from 256 to 1024) preceded by 3 CHESS pulses for water suppression.

body tissues in relation to the well known altered glycolysis of tumor cells. The biochemical behavior of FDG can be summarized as follow: it is transported into cells and phosphorylated by the same enzyme (hexokinase) acting on glucose but, unlike glucose, it cannot be further processed along the glycolytic pathway in most tissues, including tumors; therefore, phosphorylated FDG is metabolically trapped in the cell. However, the normal physiological uptake of FDG in certain tissues (as bowel) and its excretion through the renal system may alter the diagnostic accuracy of FDG-PET and limit the application of this method to malignancies in the abdomen and pelvis. Besides the general precautions adopted for PET imaging, specific patient preparation procedures are therefore suggested for imaging these regions.

Other radiotracers, which characterize tumor biology on the basis of metabolic patterns different from glucose accumulation, are under active research. Table 1 summarizes their main features and applications for breast and/or ovary cancer imaging.

Although innovative tracers move slowly to the clinic, they present some important advantages as compared to FDG, because they are able to probe metabolic pathways more specifically connected with the disease of interest and,

accordingly, are expected to be more accurate in early diagnosis or in therapy response evaluation. Furthermore, in the vast majority, these radiotracers are not physiologically excreted through the kidneys and bladder and therefore appear more suited for evaluating a local disease in the pelvis.

Finally, in recent years, there has been an improvement in instrumentation [103-106] and recent studies have focused on the added value of the dual PET/CT modality. Fused PET and CT images provide oncologists with two pieces of critical information within a single session, i.e. both the extent of viable tumor and its exact location. Initial studies in patients with different tumor types have confirmed that PET/CT both in pretreatment planning and in follow-up evaluations has a significant impact on radiotherapy management in lung and in head and neck cancer. Evaluation of PET/CT for radiation treatment planning is still in its nascent stage, still lacking rigorous randomized trials, but the method certainly shows an early promise [109].

Clinical Applications to Breast and Ovary Cancer

As summarized in Table 1, FDG-PET has now entered the clinical practice and its use in breast cancer can be very helpful in many common situations. The major areas of

Table 1. Tracers Currently Used in Breast and/or Ovary Cancer PET Imaging^a

Metabolite (analog)	Isotope ^b	Use in breast cancer	Use in ovary cancer
Energy metabolism			
Fluorodeoxyglucose (FDG)	¹⁸ F	Most frequently used. Approved by CMS ^c as an adjunct for staging in patients with distant metastasis or locoregional recurrence and for monitoring tumor response to treatment	Most frequently used in primary staging and recurrence detection
DNA metabolism (cellular proliferation)			
Thymidine	¹¹ C	No data	Limited studies
Fluorothymidine (FLT)	¹⁸ F	Limited studies	No data
Protein metabolism (amino acid transport and metabolism)			
Methionine	¹¹ C	Limited studies	Limited studies in primary staging
Cell membrane uptake (cellular proliferation)			
Choline	¹¹ C/ ¹⁸ F	Limited studies at preclinical level	Limited studies in primary staging
More specific tracers			
16 α -Fluoroestradiol (FES)	¹¹ C	For assessment of anti-estrogen response	No data

^a The majority of information is reviewed for ovary cancer in ref [107] and for breast cancer in ref [105] and [108].

^b Half-life: ¹⁸F = 110 min; ¹¹C = 20 min.

^c CMS = Centers for Medicare & Medicaid Services.

application and the limits of this method in initial diagnosis are excellently described in recent reviews [105, 108]. In summary, initial diagnosis of invasive breast cancer is possible with an overall specificity of 92%, but false-positives do occur in some benign inflammatory conditions and in fibroadenoma; the sensitivity varied in different studies between 84% and 93%. In addition, several studies have shown that the breast tumor size significantly affects FDG-PET scan results, the sensitivity for tumors smaller than 1 cm being 57%, as compared with 91% for tumors larger than 1 cm. Improvements in spatial resolution and scanner sensitivity are needed to increase the accuracy of diagnosis. The performance of FDG-PET imaging in breast cancer staging is different depending on the site of regional lymph nodes. The axillary lymph node involvement was initially detected with a 85-90% of sensitivity; however, in a more recent series of studies with a larger fraction of T1 primary tumors, a situation more similar to the typical screened populations, the sensitivity dropped to a level as low as 50%. In contrast to the mixed results of FDG-PET in axillary lymph node staging, PET resulted to be consistently useful in assessing disease spread to the internal mammary chain and mediastinal lymph nodes, which are important prognostic factors in patient management.

A review article suggests that PET, in its current format, cannot replace sentinel node biopsy but, due to its high specificity, may be useful in determining the extent of local and systemic disease [110]. Furthermore, an accurate meta-analysis estimated the pooled sensitivity, false positive rate, and the maximum joint sensitivity and specificity of the diagnostic performance of FDG-PET in the evaluation of breast cancer recurrence and metastases. The pooled sensi-

tivity was 90% (95% confidence interval 86.8-93.2) and the pooled false positive rate was 11% (95% confidence interval 7.8-14.6) after the exclusion of outliers, indicating that FDG-PET is a valuable tool for detecting breast cancer recurrence and metastases [111].

Finally, recent reports of PET or PET/CT imaging with less used or even new tracers indicate the possibility to open new avenues for future clinical usage at least in some specific areas, such as evaluation of bone metastases in patients with prostate and breast cancer by ¹⁸F-choline [36]; early identification of responders to chemotherapeutic treatments with ¹⁸F-FLT [105, 108, 112]; assessment of the response to endocrine treatment by ¹⁸F-FES [113]; and determination of the presence of cell-surface receptors suitable for following targeted therapies by engineered antibody fragments labeled with ⁶⁴Cu or ¹²⁴I [108]. However, prospective studies with large patient groups will be essential to define the exact diagnostic role of these approaches in different clinical settings.

Following some pioneering studies in early 1990's [114, 115] PET has also been more widely applied as imaging procedure for primary diagnosis and detection of ovary cancer recurrence [reviewed in 107, 116]. Although excretion through the urinary tract could limit ¹⁸F-FDG application for detecting tumors in the pelvis, most of studies have been performed with this tracer. The major conclusions of recent reviews are that ¹⁸F-FDG-PET has limited value in early diagnosis, while, due to its high sensitivity and specificity, can be useful in identifying patients with suspected recurrent tumor. In addition, in both the female and male reproductive tract, whole body imaging with FDG-PET is

capable of visualizing lymph-node and distant metastases before these changes become apparent on conventional cross-sectional imaging modalities [117].

Only few authors attempted ovary cancer PET imaging with alternative tracers, such as ^{11}C -Methionine [115] and ^{11}C -Choline [118]; the relative advantage of only minimal radioactivity in the urinary tract and bladder was counter-balanced by a variable background activity in the intestine and the shorter time-frame for image acquisition due to the very short ^{11}C half-life. Available studies are still limited by the relatively low number of patients and wide confidence intervals of the analysis, thus no conclusion about suitability of different tracers could be drawn.

Despite the present limitations, due to the rapid progress in molecular imaging, the development of new tracers and the increased knowledge in tumor metabolism, PET, either alone or in combination with CT, is expected in the near future to enter the routine clinical practice for detecting ovarian cancer recurrence and early response to treatment. In this framework, Cho-PET may provide important contributions, especially in view of the high level of uptake of radiolabeled choline in human ovary cancer cells [15].

CONCLUSIONS AND FUTURE DIRECTIONS

The continuous progress in characterizing features and mechanisms of altered choline metabolism in tumor cells may lead to improvements in the effectiveness of noninvasive imaging methods such as MRS and Cho-PET in cancer diagnosis and therapy response follow-up.

^1H -MRS studies conducted on breast and ovary cancer cells provided acquisition of an integrated set of information on altered choline metabolism during tumor progression. The tCho pool may reach in these cancer cells concentrations as high as 4 to 7 mM, PCho representing the most abundant component ($80 \pm 10\%$). Both biosynthetic and degradative PC-cycle enzymes likely contribute to the increased PCho levels.

^1H -MRS of the breast is on the way of converting from a role of a research tool to that of a possible clinical tool. Open problems are: i) sequence optimization, to obtain spectra with a good S/N ratio also for lesions less than 10 mm in diameter; ii) post-processing standardization with a higher spectral resolution within the tCho peak; iii) absolute quantification of tCho concentration in tumor tissues. Acquisition of metabolic maps of the breast using 3D multi-voxel MRS imaging approaches are expected to provide powerful means to integrate anatomical and biochemical information at the clinical level.

The new body of evidence specifically acquired on altered choline metabolism in ovary cancer cells warrants further efforts to elucidate the value of integrating the current imaging modalities with the metabolic information provided by ^1H -MRS and Cho-PET approaches, to improve the strategies of noninvasive diagnosis and therapy response follow-up.

ACKNOWLEDGEMENTS

The broad scope of this review has necessitated citation of only representative examples throughout. We apologize to

numerous investigators whose excellent work has not been cited.

Grants by a Special Project of the Italian Health Ministry (2001) and by Cassa di Risparmio delle Provincie Lombarde Foundation (CARIPLO) are gratefully acknowledged.

The Authors are indebted to Dr. Filippo Belardelli, Dr. Carmen Rozera, Mr. Massimo Spada and Mr. Massimo Giannini (Istituto Superiore di Sanità, Roma) and to Dr. Andrea Iozzelli (Unit of Radiology, IRCCS Policlinico San Donato Milanese) for collaboration in experimental and clinical examinations.

REFERENCES

- [1] Negendank WG. Studies of human tumors by MRS: a review. *NMR Biomed* 1992; 5: 303-24.
- [2] de Certaines JD, Larsen VA, Podo F, Carpinelli G, Briot O, Henriksen O. *In vivo* ^{31}P MRS of experimental tumours. *NMR Biomed* 1993; 6: 345-65.
- [3] Podo F. Tumour phospholipid metabolism. Review article. *NMR Biomed* 1999; 12: 413-39.
- [4] Ackerstaff E, Glunde K, Bhujwala ZW. Choline phospholipid metabolism: a target in cancer cells? *J Cell Biochem* 2003; 90: 525-33.
- [5] Glunde K, Ackerstaff E, Mori N, Jacobs MA, Bhujwala ZM. Choline phospholipid metabolism in cancer: consequences for molecular pharmaceutical interventions. *Mol Pharm* 2006; 3: 496-506.
- [6] Aboagye EO, Bhujwala ZM. Malignant transformation alters membrane choline phospholipid metabolism of human mammary epithelial cells. *Cancer Res* 1999; 59: 80-4.
- [7] Katz-Brull R, Seger D, Rivenson-Segal D, Rushkin E, Degani H. Metabolic markers of breast cancer: enhanced choline metabolism and reduced choline-ether-phospholipid synthesis. *Cancer Res* 2002; 62:1966-70.
- [8] Tse GM, Yeung DK, King AD, Cheung HS, Yang WT. *In vivo* proton magnetic resonance spectroscopy of breast lesions: an update. *Breast Cancer Res Treat* 2006 Oct 19 [Epub ahead of print].
- [9] Ackerstaff E, Pflug BR, Nelson JB, Bhujwala ZM. Detection of increased choline compounds with proton nuclear magnetic resonance spectroscopy subsequent to malignant transformation of human prostatic epithelial cells. *Cancer Res* 2001; 61: 3599-603.
- [10] Chen AP, Cunningham CH, Kurhanewicz J, et al. High-resolution 3D MR spectroscopic imaging of the prostate at 3 T with the MLEV-PRESS sequence. *Magn Reson Imaging* 2006; 24: 825-32.
- [11] Mori N, Delsite R, Natarajan K, Kulawiec M, Bhujwala ZM, Singh KK. Loss of p53 function in colon cancer cells results in increased phosphocholine and total choline. *Mol Imaging* 2004; 3: 319-23.
- [12] Wang CK, Li CW, Hsieh TJ, Chien SH, Liu GC, Tsai KB. Characterization of bone and soft-tissue tumors with *in vivo* ^1H MR spectroscopy: initial results. *Radiology* 2004; 232: 599-605.
- [13] Stadlbauer A, Gruber S, Nimsky C, et al. Preoperative grading of gliomas by using metabolite quantification with high-spatial-resolution proton MR spectroscopic imaging. *Radiology* 2006; 3: 958-69.
- [14] Ferretti A, D'Ascenzo S, Knijn A, Iorio E, Dolo V, Podo F. Detection of polyol accumulation in a new ovarian carcinoma cell line, CABA 1: a ^1H NMR study. *Br J Cancer* 2002; 86: 1180-87.
- [15] Iorio E, Mezzanzanica D, Alberti P, et al. Alterations of choline phospholipid metabolism in ovarian tumor progression. *Cancer Res* 2005; 65: 9369-76.
- [16] Pelech SL, Vance DE. Signal transduction via phosphatidylcholine cycles. *Trends Biochem Sci* 1989; 14: 28-30.
- [17] Glunde K, Serkova NJ. Therapeutic targets and biomarkers identified in cancer choline phospholipid metabolism. *Pharmacogenomics* 2006; 7: 1109-23.
- [18] <http://www.imaginis.com/breasthealth/statistics.asp>
- [19] Kamangar F, Dores GM, Anderson WF. Patterns of cancer incidence, mortality, and prevalence across five continents: defining priorities to reduce cancer disparities in different geographic regions of the world. *J Clin Oncol* 2006; 24: 2137-50.

- [20] Pusztai L, Mazouni C, Anderson K, Wu Y, Symmans WF. Molecular classification of breast cancer: limitations and potential. *Oncologist* 2006; 11: 868-77.
- [21] Kuhl CK, Kuhn W, Schild H. Management of women at high risk for breast cancer: new imaging beyond mammography. *Breast* 2005; 14: 480-6.
- [22] Leach MO, Boggis CR, Dixon AK, *et al.* Screening with magnetic resonance imaging and mammography of a UK population at high familial risk of breast cancer: a prospective multicentre cohort study (MARIBS). *Lancet* 2005; 365: 1769-78.
- [23] Sardanelli F, Podo F, D'Agnolo G, *et al.* Multicenter comparative multimodality surveillance of women at genetic-familial high risk of breast cancer: Interim results. *Radiology*, (published online before print January 23, 2007).
- [24] Sardanelli F, Podo F. Breast MR imaging in women at high-risk of breast cancer. Is something changing in early breast cancer detection? *Eur Radiol* 2006 Sep 29 [Epub ahead of print]
- [25] Koutcher JA, Goldsmith M, Damadian R. NMR in cancer. X. A malignancy index to discriminate normal and cancerous tissue. *Cancer* 1978; 41: 174-82.
- [26] Heywang SH. Status of research in the field of diagnostic imaging of the breast with particular reference to magnetic resonance tomography. *Röntgenpraxis* 1988; 41: 384-94.
- [27] Heywang SH, Hahn D, Schmidt H, *et al.* MRI of the breast using gadolinium-DTPA. *J Comput Assist Tomogr* 1986; 10: 199-204.
- [28] Vomweg TW, Buscema M, Kauczor HU, *et al.* Improved artificial neural networks in prediction of malignancy of lesions in contrast-enhanced MR-mammography. *Med Phys* 2003; 30: 2350-9.
- [29] Kuhl CK, Schild HH, Morakkabati N. Dynamic bilateral contrast-enhanced MR imaging of the breast: trade-off between spatial and temporal resolution. *Radiology* 2005; 236: 789-800.
- [30] Payne GS, Dowsett M, Leach MO. Hormone-dependent metabolic changes in the normal breast monitored noninvasively by ^{31}P magnetic resonance (MR) spectroscopy. *Breast* 1994; 3: 20-3.
- [31] Park JM, Park JH. Human *in-vivo* ^{31}P MR spectroscopy of benign and malignant breast tumors. *Korean J Radiol* 2001; 2: 80-6.
- [32] Mountford CE, Doran S, Lean CL, Russell P. Proton MRS can determine the pathology of human cancers with a high level of accuracy. *Chem Rev* 2004; 104: 3677-704.
- [33] Pathak AP, Gimi B, Glunde K, Ackersstaff E, Artemov D, Bhujwala ZM. Molecular and functional imaging of cancer: advances in MRI and MRS. *Methods Enzymol.* 2004; 386: 3-60.
- [34] Gillies RJ, Morse DL. *In vivo* magnetic resonance spectroscopy in cancer. *Annu Rev Biomed Eng* 2005; 7: 287-326.
- [35] Tosi R and Tugnoli V Eds, *Nuclear Magnetic Resonance Spectroscopy in the study of neoplastic tissue*. New York, Nova Science Publisher, Inc. 2005.
- [36] Langsteger W, Heinisch M, Fogelman I. The role of fluorodeoxyglucose, ^{18}F -dihydroxyphenylalanine, ^{18}F -choline and ^{18}F -fluoride in bone imaging with emphasis on prostate and breast. *Sem Nucl Med* 2006; 36: 73-92.
- [37] Parkin DM, Whelan SL, Ferlay J, Teppo L, Thomas DB. Cancer incidence in five continents. VIII. Lyon (France): IARC Press; 2002.
- [38] Jemal A, Siegel R, Ward E, *et al.* Cancer statistics, 2006. *CA Cancer J Clin* 2006; 56: 106-30.
- [39] Bell DA. Origins and molecular pathology of ovarian cancer. *Mod. Pathol* 2005; 18 Suppl 2: S19-S32.
- [40] Canevari S, Gariboldi M, Reid JF, Bongarzone I, Pierotti MA. Molecular predictors of response and outcome in ovarian cancer. *Crit Rev Oncol Hematol* 2006; 60: 19-37.
- [41] Shih IeM, Kurman RJ. Ovarian tumorigenesis: a proposed model based on morphological and molecular genetic analysis. *Am J Pathol* 2004; 164: 1511-8.
- [42] Classe JM, Fontanelli R, Bischof-Delaloye A, Chatal JF. Ovarian cancer management. Practice guidelines for nuclear physicians. *Q J Nucl Med Mol Imaging* 2004; 48: 143-9.
- [43] Coakley FV. Staging ovarian cancer: role of imaging. *Radiol Clin North Am* 2002; 40: 609-36.
- [44] Imaoka I, Wada A, Kaji Y, *et al.* Developing an MR imaging strategy for diagnosis of ovarian masses. *Radiographics* 2006; 26: 1431-48.
- [45] Low RN, Duggan B, Barone RM, Saleh F, and Song SYT. Treated ovarian cancer: MR imaging, laparotomy reassessment, and serum CA-125 values compared with clinical outcome at 1 year. *Radiology* 2005; 235: 918-26.
- [46] Delbeke D, Martin WH. Positron emission tomography imaging in oncology. *Radiol Clin North Am* 2001; 39: 883-917.
- [47] Sironi S, Messa C, Mangili G, *et al.* Integrated FDG PET/CT in patients with persistent ovarian cancer: correlation with histological findings. *Radiology* 2004; 433-40.
- [48] Nanni C, Rubello D, Farsad M, *et al.* (18)F-FDG PET/CT in the evaluation of recurrent ovarian cancer: a prospective study on forty-one patients. *Eur J Surg Oncol* 2005; 31: 792-7.
- [49] Reinhardt MJ, Matthiws A, Biersack HJ. PET-imaging in tumors of the reproductive tract. *Q J Nucl Med* 2002; 46: 105-12.
- [50] Bhakoo KK, Williams SR, Florian CL, Land H, Noble MD. Immortalization and transformation are associated with specific alterations in choline metabolism. *Cancer Res* 1996; 20: 4630-5.
- [51] Gribbestad IS, Sitter B, Lundgren S, Krane J, Axelsson D. Metabolite composition in breast tumors examined by proton nuclear magnetic resonance spectroscopy. *Anticancer Res* 1999; 19: 1737-46.
- [52] Vance JE and Vance DE. Phospholipid biosynthesis in mammalian cells. *Biochem Cell Biol* 2004; 82: 113-28.
- [53] Warden CH, Friedkin M. Regulation of phosphatidylcholine biosynthesis by mitogenic growth factors. *Biochim Biophys Acta* 1984; 792: 270-80.
- [54] Macara IG. Elevated phosphocholine concentration in ras-transformed NIH 3T3 cells arises from increased choline kinase activity, not from phosphatidylcholine breakdown *Mol Cell Biol* 1989; 9: 325-8.
- [55] Ramirez de Molina A, Rodriguez-Gonzalez A, Gutierrez R, *et al.* Overexpression of choline kinase is a frequent feature in human tumor-derived cell lines and in lung, prostate, and colorectal human cancers. *Biochem Biophys Res Commun* 2002; 296: 580-3.
- [56] Ramirez de Molina A, Gutierrez R, *et al.* Increased choline kinase activity in human breast carcinomas: clinical evidence for a potential novel antitumor strategy. *Oncogene* 2002; 21: 4317-22.
- [57] Al-Saffar NM, Troy H, Ramirez de Molina A, *et al.* Non invasive magnetic resonance spectroscopic pharmacodynamic markers of the choline kinase inhibitor MN58b in human carcinoma models. *Cancer Res* 2006; 66: 427-34.
- [58] Ramirez de Molina AR, Banez-Coronel M, Gutierrez R, *et al.* Choline kinase activation is a critical requirement for the proliferation of primary human mammary epithelial cells and breast tumor progression. *Cancer Res* 2004; 64: 6732-9.
- [59] Glunde K, Raman V, Mori N, Bhujwala ZM. RNA interference-mediated choline kinase suppression in breast cancer cells induces differentiation and reduces proliferation. *Cancer Res* 2005; 65: 11034-43.
- [60] Aoyama C, Liao H, Ishidate K. Structure and function of choline kinase isoforms in mammalian cells. *Progr Lipid Res* 2004; 43: 266-81.
- [61] Lacal JC. Choline kinase: a novel target for antitumor drugs. *IDrugs* 2001; 4: 419-26.
- [62] Yoshimoto M, Waki A, Obata A, Furukawa T, Yonekura Y, Fujibayashi Y. Radiolabeled choline as a proliferation marker: comparison with radiolabeled acetate. *Nucl Med Biol* 2004; 31: 859-65.
- [63] DeGrado TR, Baldwin SW, Wang S, *et al.* Synthesis and evaluation of (18)F-labeled choline analogs as oncologic PET tracers. *J Nucl Med* 2001; 42: 1805-14.
- [64] Hara T. ^{18}F -Fluorocholine: a new oncologic PET tracer. *J Nucl Med* 2001; 42: 1815-17.
- [65] Podo F, Carpinelli G, Ferretti A, Borghi P, Proietti E, Belardelli F. Activation of glycerophosphocholine phosphodiesterase in Friend leukemia cells upon *in vitro*-induced erythroid differentiation. ^{31}P and ^1H NMR studies. *Israel J Chem* 1992; 32: 47-54.
- [66] Gribbestad IS, Singstad TE, Nilsen G, *et al.* *In vivo* ^1H MRS of normal breast and breast tumors using a dedicated double breast coil. *J Magn Reson Imaging* 1998; 8: 1191-7.
- [67] Roebuck JR, Cecil KM, Schnall MD, Lenkinski RE. Human breast lesions: characterization with proton MR spectroscopy. *Radiology* 1998; 209: 269-75.
- [68] Kvstad KA, Bakken IJ, Gribbestad IS, *et al.* Characterization of neoplastic and normal human breast tissues with *in vivo* ^1H MR spectroscopy. *J Magn Reson Imaging* 1999; 10: 159-64.
- [69] Yeung DK, Cheung HS, Tse GM. Human breast lesions: characterization with contrast-enhanced *in vivo* proton MR spectroscopy - Initial results. *Radiology* 2001; 220: 40-6.

- [70] Jagannathan NR, Kumar M, Seenu V, *et al.* GK. Evaluation of total choline from *in-vivo* volume localized proton MR spectroscopy and its response to neoadjuvant chemotherapy in locally advanced breast cancer. *Br J Cancer* 2001; 84:1016-22.
- [71] Bakken IJ, Gribbestad IS. External standard method for the *in vivo* quantification of choline-compounds in breast tumors by proton MR spectroscopy at 1.5 T. *proton MR spectroscopy at 1.5 Tesla*. *Magn Reson Med* 2001; 46: 189-92.
- [72] Cecil KM, Schnall MD, Siegelman ES, Lenkinski RE. The evaluation of human breast lesions with magnetic resonance imaging and proton magnetic resonance spectroscopy. *Breast Cancer Res Treat* 2001; 68: 45-54.
- [73] Katz-Brull R, Lavin PT, Lenkinski RE. Clinical utility of proton magnetic resonance spectroscopy in characterizing breast lesions. *J Natl Cancer Inst* 2002; 94: 1197-203.
- [74] Tse GM, Cheung HS, Pang LM, *et al.* Characterization of lesions of breast with proton MR spectroscopy: comparison of carcinomas, benign lesions, and phyllodes tumors. *AJR Am J Roentgenol* 2003; 181: 1267-72.
- [75] Kim JK, Park SH, Lee HM, *et al.* *In vivo* ¹H-MRS evaluation of malignant and benign breast diseases. *Breast* 2003; 12: 179-82.
- [76] Bolan PJ, Meisamy S, Baker EH, *et al.* *In vivo* quantification of choline compounds in the breast with ¹H MR spectroscopy. *Magn Reson Imaging* 2003; 50: 1134-43.
- [77] Huang W, Fisher PR, Dulaimy K, Tudorica LA, O'Hea B, Button TM. Detection of breast malignancy: diagnostic MR protocol for improved specificity. *Radiology* 2004; 232: 585-91.
- [78] Jacobs MA, Barker PB, Bottomley PA, Bhujwalla Z, Blumke DB. Proton MR spectroscopic imaging of human breast cancer: A preliminary study. *J Magn Reson Imaging* 2004; 19: 68-75.
- [79] Stanwell P, Gluch L, Clark D, *et al.* Specificity of choline metabolites for *in vivo* diagnosis of breast cancer using ¹H MRS at 1.5 T. *Eur Radiol* 2005; 15: 1037-43.
- [80] Meisamy S, Bolan PJ, Baker EH, *et al.* Adding *in vivo* quantitative ¹H MR spectroscopy to improve diagnostic accuracy of breast MR imaging: preliminary results of observer performance study at 4.0 T. *Radiology* 2005; 236: 465-75.
- [81] Jacobs MA, Barker PB, Argani P, Ouwerkerk R, Bhujwalla ZM, Blumke DA. Combined dynamic contrast enhanced breast MR and proton spectroscopic imaging: a feasibility study. *J Magn Reson Imaging* 2005; 21: 23-8.
- [82] Bartella L, Morris EA, Dershaw DD, *et al.* Proton spectroscopy with choline peak as malignancy marker improves positive predictive value for breast cancer diagnosis: Preliminary study. *Radiology* 2006; 239: 686-92.
- [83] Yeung DK, Yang WT, Tse GM. Breast cancer: *in vivo* proton MR spectroscopy in the characterization of histopathologic subtypes and preliminary observations in axillary node metastases. *Radiology* 2002; 225: 190-7.
- [84] Sharma U, Mehta A, Seenu V, Jagannathan NR. Biochemical characterization of metastatic lymph nodes of breast cancer patients by *in vitro* ¹H magnetic resonance spectroscopy: a pilot study. *Magn Reson Imaging* 2004; 22: 697-706.
- [85] Seenu V, Pavan Kumar MNP, Sharma U, Gupta SD, Mehta SN, Jagannathan NR. Potential of magnetic resonance spectroscopy to detect metastasis in axillary lymph nodes in breast cancer. *Magn Reson Imaging* 2005; 23: 1005-10.
- [86] Salibi N, Brown MA. *Clinical MR spectroscopy. First principles*. New York: Wiley-Liss, 1998: 75-80.
- [87] Gribbestad IS, Peterson SB, Fjone HE, Kvinnsland S, Krane J. ¹H NMR spectroscopic characterization of perchloric acid extracts from breast carcinomas and non-involved breast tissue. *NMR Biomed* 1994; 7: 181-194.
- [88] MacKinnon WB, Barry PA, Malycha PL, *et al.* Fine-needle biopsy specimens of benign breast lesions distinguished from invasive cancer *ex vivo* with proton MR spectroscopy. *Radiology* 1997; 204: 661-6.
- [89] Cheng LL, Chang IW, Smith BL, Gonzales RG. Evaluation of human breast ductal carcinoma with high-resolution magic-angle spinning proton magnetic resonance spectroscopy. *J Magn Reson* 1998; 135: 194-202.
- [90] Sitter B, Sonnewald U, Spraul M, Fjösne HE, Gribbestad IS. High-resolution magic angle spinning HR MAS of breast cancer tissue. *NMR Biomed* 2002; 15: 327-37.
- [91] Fitch WL, Detre G., Holmes CP, Shoolery JN, Keifer P. High resolution ¹H NMR in solid phase organic synthesis. *J Org Chem* 1994; 59: 7955-56.
- [92] Bathen TF, Jensen LR, Sitter B, *et al.* MR-determined metabolic phenotype of breast cancer in prediction of lymphatic spread, grade, and hormone status. *Breast Cancer Res Treat* 2006; Oct 24 [Epub ahead of print].
- [93] American College of Radiology. Reporting system. In: *Breast Imaging Reporting and data System (BI-RADS)*. 3rd ed. Reston, VA: American College of Radiology, 1998.
- [94] Wallace JC, Raaphorst GP, Somorjai RL, *et al.* Classification of ¹H MR spectra of biopsies from untreated and recurrent ovarian cancer using linear discriminant analysis. *Magn Reson Med* 1997; 38: 569-76.
- [95] Smith JC, Blandford DE. Diagnosis of cancer in humans by ¹H NMR of tissue biopsies. *Biochem Cell Biol* 1998; 76: 472-476.
- [96] Boss EA, Moolenaar SH, Massuger LF, *et al.* High-resolution proton nuclear magnetic resonance spectroscopy of ovarian cyst fluid. *NMR Biomed* 2000; 13: 297-305.
- [97] Okada T, Harada M, Matsuzaki K, Nishitani H, Aono T. Evaluation of female intrapelvic tumors by clinical proton MR spectroscopy. *J Magn Reson Imaging* 2001; 13: 912-7.
- [98] Hascalik S, Celik O, Sarac K, Meydanli MM, Alkan A, Mizrak B. Metabolic changes in pelvic lesions: findings at proton MR spectroscopic imaging. *Gynecol Obstet Invest* 2005; 60: 121-7.
- [99] Rofstad EK, DeMuth P, Sutherland RM. ³¹P NMR spectroscopy measurements of human ovarian carcinoma xenografts: relationships to tumor volume, growth rate, necrotic fraction and differentiation status. *Radiother Oncol* 1988; 12: 315-26.
- [100] Klostergaard J, Auzenne E, Ghosh S, Farquhar D, Rivera B, Price RE. Magnetic resonance imaging-based prospective detection of intraperitoneal human ovarian carcinoma xenografts treatment response. *Int J Gynecol Cancer* 2006; 16 Suppl 1: 111-7.
- [101] Han LY, Landen CN, Trevino JG, *et al.* Antiangiogenic and antitumor effects of SRC inhibition in ovarian carcinoma. *Cancer Res* 2006; 66: 8633-9.
- [102] Kim KS, Sengupta S, Berk M, *et al.* Hypoxia Enhances Lysophosphatidic Acid Responsiveness in ovarian cancer cells and lysophosphatidic acid induces ovarian tumor metastasis *in vivo*. *Cancer Res* 2006; 66: 7983-90.
- [103] Kumar R, Nadig MR, Chauhan A. Positron emission tomography: clinical applications in oncology. Part 1. *Expert Rev Anticancer Ther* 2005; 5: 1079-94.
- [104] Kumar R, Chauhan A. Positron emission tomography: clinical applications in oncology. Part 2. *Expert Rev Anticancer Ther* 2006; 6: 625-40.
- [105] Mankoff DA, Eubank WB. Current and future use of positron emission tomography (PET) in breast cancer. *J Mammary Gland Biol Neoplasia* 2006; 11: 125-136.
- [106] Jager PL, de Korte MA, Lub-de Hooge MN, *et al.* Molecular imaging: what can be used today. *Cancer Imaging* 2005; 5 Spec No A: S27-32.
- [107] Kumar R, Chauhan A, Jana S, Dadparvar S. Positron emission tomography in gynecological malignancies. *Expert Rev Anticancer Ther* 2006; 6: 1033-44.
- [108] Quon A, Gambhir SS. FDG-PET and beyond: molecular breast cancer imaging. *J Clin Oncol* 2005; 23: 1664-73.
- [109] Messa C, Di Muzio N, Picchio M, Gilardi MC, Bettinardi V, Fazio F. PET/CT and radiotherapy. *Q J Nucl Med Mol Imaging* 2006; 50: 4-14.
- [110] Guller U, Nitzsche E, Moch H, Zuber M. Is positron emission tomography an accurate non-invasive alternative to sentinel lymph node biopsy in breast cancer patients?. *J Natl Cancer Inst* 2003; 95: 1040-3.
- [111] Isasi CR, Moadel RM, Blaufox MD. A meta-analysis of FDG-PET for the evaluation of breast cancer recurrence and metastases. *Breast Cancer Res Treat* 2005; 90: 105-12.
- [112] Been LB, Elsinga PH, de Vries J, *et al.* Positron emission tomography in patients with breast cancer using ¹⁸F-3'-deoxy-3'-fluoro-l-thymidine (¹⁸F-FLT)-a pilot study. *Eur J Surg Oncol* 2006; 32: 39-43.
- [113] Linden HM, Stekhova SA, Link JM, *et al.* Quantitative fluoroestradiol positron emission tomography imaging predicts response to endocrine treatment in breast cancer. *J Clin Oncol* 2006; 24: 2793-9.

- [114] Hubner KF, McDonald TW, Niethammer JG, Smith GT, Gould HR, Buonocore E. Assessment of primary and metastatic ovarian cancer by positron emission tomography (PET) using 2- ^{18}F deoxyglucose (2- ^{18}F FDG). *Gynecol Oncol* 1993; 51: 197-204.
- [115] Lapela M, Leskinen-Kallio S, Varpula M, *et al.* Metabolic imaging of ovarian tumors with carbon-11-methionine: a PET study. *J Nucl Med* 1995; 36: 2196-200.
- [116] Havrilesky LJ, Kulasingam SL, Matchar DB, Myers ER. FDG-PET for management of cervical and ovarian cancer. *Gynecol Oncol* 2005; 97: 183-91.
- [117] Reinhardt MJ, Matthies A, Biersack HJ. PET-imaging in tumors of the reproductive tract. *Q J Nucl Med* 2002; 46: 105-12.
- [118] Torizuka T, Kanno T, Futatsubashi M, *et al.* Imaging of gynecologic tumors: comparison of ^{11}C -choline PET with ^{18}F -FDG PET. *J Nucl Med* 2003; 44: 1051-6.